Revista de Metalurgia
Vol. 53, Issue 3, July–September 2017, e098
ISSN-L: 0034-8570
http://dx.doi.org/10.3989/revmetalm.098

Electrical properties of ternary Bi-Ge-Sb and Al-Cu-Sb alloys

Milena Premovic[a,✉], Duško Minić[a], Milan Kolarevic[b], Dragan Manasijevic[c], Dragana Živković[c, †], Aleksandar Djordjevic[a], Dusan Milisavljevic[a]

[a] University in Priština, Faculty of Technical Science, K.M. 7, 4000 Kos. Mitrovica, Serbia
[b] University of Kragujevac, Faculty of Mechanical and Civil Engineering, Dositejeva 19, 36000 Kraljevo, Serbia
[c] University of Belgrade, Technical Faculty, VJ 12, 19210 Bor, Serbia
✉Corresponding author: milena.premovic@gmail.com
(† Deceased 26th November 2016)

Submitted: 21 March 2016; Accepted: 28 February 2017; Available On-line: 11 July 2017

ABSTRACT: Electrical properties of ternary Bi-Ge-Sb and Al-Cu-Sb alloys. This paper presents review of electrical properties of two ternary systems based on Sb, ternary Bi-Ge-Sb and Al-Cu-Sb system. Beside electrical properties in paper are presented microstructures of both systems observed with light optical microscopy. On four samples microstructural analysis was carried out by scanning electron microscopy combined with energy dispersive spectrometry and X-ray powder diffraction technique. Moreover, micro hardness of selected alloys from the ternary Bi-Ge-Sb system was determined using Vickers hardness tests.

KEYWORDS: Electrical conductivity; Hardness; Materials testing; Microstructure

Citation/Citar como: Premovic, M.; Minić, D.; Kolarevic, M.; Manasijevic, D.; Živković, D.; Djordjevic, A.; Milisavljevic, D. (2017) "Electrical properties of ternary Bi-Ge-Sb and Al-Cu-Sb alloys". *Rev. Metal.* 53(3): e098. http://dx.doi.org/10.3989/revmetalm.098

RESUMEN: *Propiedades eléctricas de las aleaciones ternarias Bi-Ge-Sb y Al-Cu-Sb.* Este artículo presenta el estudio de las propiedades eléctricas de dos sistemas ternarios basados en antimonio, Bi-Ge-Sb y Al-Cu-Sb. Además de las propiedades eléctricas, en el artículo se presenta las microestructuras observadas por microscopía óptica. Se utilizaron cuatro muestras para el análisis de la microestructura utilizando MEB, EDS y DRX. Además, se determinó la microdureza de muestras seleccionadas de la aleación ternaria Bi-Ge-Sb, la dureza se determinó utilizando ensayos Vickers.

PALABRAS CLAVE: Conductividad eléctrica; Dureza; Materiales de muestra; Microestructura

ORCID ID: Milena Premovic (http://orcid.org/0000-0003-0532-7048); Duško Minić (http://orcid.org/0000-0002-0432-6038); Milan Kolarevic (http://orcid.org/0000-0001-6521-5035); Dragan Manasijevic (http://orcid.org/0000-0002-7828-8994); Dragana Živković (http://orcid.org/0000-0002-2745-5676); Aleksandar Djordjevic (http://orcid.org/0000-0002-5136-7019); Dusan Milisavljevic (http://orcid.org/0000-0003-0598-2392)

1. INTRODUCTION

Antimony is an important metal in the world economy because of the applications in many industries, such as electronics industry, military industry, pharmaceutical industry, etc. (Vinhal *et al.*, 2016). The largest producer of antimony is China with 114 Sb mines and approximately 90% of the world's production (He *et al.*, 2012; Sun *et al.*, 2016). The other producers are Canada, Russia, Bolivia and South Africa.

In the electronics industry antimony is used for making semiconductor devices, such as infrared detectors and diodes (Serrano *et al.*, 2016). Antimony compounds are used to make bullets (Johnson *et al.*, 2005), flame-retardant materials, car brake liner lubricants, type metal (in printing presses), enamels, cable sheathing, catalysts for the production of polyethylene terephthalate (PET) and alloy additives glass and pottery (Bech *et al.*, 2012; Cui *et al.*, 2015; Macgregor *et al.*, 2015). On the other hand antimony is used as a medicine in the treatment of Leishmaniasis and their potential usefulness in AIDS and cancer therapy (Pierart *et al.*, 2015).

Beside wide application of antimony it is important to study different combination of antimony with other element. During the past decades so many combination and also different composition of binary systems based on Sb were studied (Liu *et al.*, 2013; Gierlotka, 2014) and later ternary systems (Zobač *et al.*, 2015; Guo *et al.*, 2016).

These two ternary systems Al-Cu-Sb and Bi-Ge-Sb were investigated before by the same group of authors as this paper. The ternary Al-Cu-Sb system was previously investigated by Minić *et al.* (2013) who experimentally studied liquid surface, three vertical sections and two isothermal sections at 200 °C and 400 °C. Another ternary Bi-Ge-Sb system was investigated by Premovic *et al.* (2014). In the paper given by Premovic *et al.* (2014) are investigated liquid projection, invariant reactions, three vertical sections, as well as isothermal sections at 100 °C and 500 °C.

In this paper electrical properties and microstructure of the alloy samples from the ternary Al-Cu-Sb and Bi-Ge-Sb systems are presented. Beside mentioned properties results of SEM-EDS and XRD measurement are presented as well. Also micro hardness was determined for some alloys from ternary Bi-Ge-Sb system. This kind of paper or similar (Illescas *et al.*, 2009; Verbeken *et al.,* 2010) will give a better insight into properties of alloys which should contribute to further development of application area.

2. MATERIALS AND METHODS

All investigated samples were prepared from high purity (99.999 at. %) element produced by Alfa Aesar (Germany) in an induction furnace under high-purity argon atmosphere. Given that Sb is highly volatile an additional amount of Sb (about 1 to 2 at. %) was added to compensate for the weight loss. Additional amount of antimony is highly recommended especially for high antimony systems. In general, the average loss of mass during melting of samples was about 1 at.%.

Microstructural analysis was carried out by TESCAN VEGA3 scanning electron microscope with energy dispersive spectroscopy (EDS) (Oxford Instruments X-act) and by light microscopy using (LOM) OLYMPUS GX41 inverted metallographic microscope. Samples were prepared by the classic metallographic procedure without etching. Polished samples were firstly subjected to EDS elemental mapping to check compositional homogeneity and possible segregation and then analyzed. Overall composition and compositions of coexisting phases was determined using EDS point and area analysis.

XRD patterns of the studied samples were recorded on a D2 PHASER powder diffractometer equipped with a dynamic scintillation detector and ceramic X-ray Cu tube (KFLCu-2K) in a 2θ range of 5° to 75° with a step size of 0.02°. The patterns were analyzed using Topas 4.2 software and ICDD databases PDF2 (2013).

As the next step, electrical conductivity and hardness measurements were performed. Electrical conductivity measurements were carried out using Foerster SIGMATEST 2.069 eddy current instrument. The microhardness of the phases present in the microstructure was determined using a Vickers microhardness tester Sinowon, model Vexus ZHV-1000V.

3. RESULTS

The alloy samples from ternary Bi-Ge-Sb system were investigated using several different techniques. Thirteen ternary alloy samples were observed with light optical microscopy, same samples were subjected to the measurement of the electrical conductivity. Further each phase detected in microstructure is subjected for determination of the microhardness. Additionally two ternary samples are investigated with XRD and SEM-EDS techniques.

Eight alloy samples from ternary Al-Cu-Sb system were observed with light optical microscopy and on same samples electrical conductivity were determined. For better insight into microstructures two ternary alloys are investigated with SEM-EDS and XRD techniques.

In Table 1 are presented list of phases for both ternary system with their corresponding Pearson symbols.

Thirteen alloy samples for investigation of electrical conductivity were selected along three vertical sections Ge-BiSb, Sb-BiGe and Bi-GeSb for ternary Bi-Ge-Sb and eight alloy samples from two

TABLE 1. Considered phases and their crystal structures for ternary Bi-Ge-Sb and Al-Cu-Sb system

Phase name	Common name	Pearson symbol	Space group
Bi-Ge-Sb system			
LIQUID	L	-	-
RHOMBO_A7	(Bi, Sb)	*hR2*	$R\bar{3}m$
DIAMOND_A4	α (Ge)	*cF8*	$Fd\bar{3}m$
Al-Cu-Sb system			
LIQUID	L	-	-
RHOMBO_A7	(Sb)	*hR2*	$R\bar{3}m$
FCC_A1	(Al, Cu)	*cF4*	$Fm\bar{3}m$
ALCU-ETA	AlCu	*mC20*	*Cm/2*
AL2CU_TYPE	Al_2Cu	*tI12*	*I4/mcm*
ALCU_DELTA	Al_2Cu_3	*hP42*	$R\bar{3}m$
ALCU_ZETA	Al_9Cu_{11}	*oI24*	Imm^2
ALCUZN_GAMMA_H	Al_5Cu_8	*cI52*	$I4\bar{3}m$
BCC_A2	Cu_3Al	*cF16*	$Fm\bar{3}m$
GAMMA_BRASS	AL_4Cu_9	*cI52*	$P4\bar{3}m$
NIAS_TYPE	$AlCu_2$	*hP6*	…
ALSB	AlSb	*cF8*	$F4\bar{3}m$
BCC_A2	Cu_3Sb	*cF16*	$Fm\bar{3}m$
CUSB_ETA	Cu_2Sb	*tP6*	*P4/nmm*
CUSB_ZETA	$Cu_{73}Sb_{20}$	*hP26*	$F\bar{3}$
CUSB_GAMMA	$Cu_{11}Sb_2$	*hP2*	$P6_3/mmc$
CUSB_DELTA	Cu_9Sb_2	*hP**	$P6_3/mmc$
CUSB_EPSILON	$Cu_{10}Sb_3$	*oP8*	*Pmmn*

vertical sections Al-CuSb and Sb-AlCu for ternary Al-Cu-Sb. The obtained values of the electrical conductivity of the studied alloy samples are given in Table 2. Also in Table 2 are presented experimentally obtained values for five binary alloys and literature value for electrical conductivity of pure elements, which are taken from online database periodictable, Electrical Conductivity of the elements (Gray *et al.*, 2013).

In comparison of the obtained experimental results of electrical conductivity given in Table 2, it is clearly visible that ternary Al-Cu-Sb alloys have a significantly higher value of the electrical conductivity than alloy from ternary Bi-Ge-Sb system.

Based on experimentally determined values of electrical conductivity given in Table 2 and using an appropriate mathematical model, electrical conductivity of all other alloys in ternary systems have been calculated.

To define a mathematical model for electric conductivity of alloys software package Design Expert v.9.0.3.1 were used. Out of possible canonical or Scheffe models (Cornell, 1990; Kolarević, 2004; Lazić, 2004) that meet the requirements of adequacy recommended is Special Quartic model, Eq. (1):

$$\hat{y}=\sum_{i=1}^{q}\beta_i x_i+\sum_{i<j}^{q-1}\sum_{j}^{q}\beta_{ij}x_i x_j+\sum_{i<j}^{q-2}\sum_{j<k}^{q-1}\sum_{k}^{q}\beta_{iijk}x_i^2 x_j x_k+\sum_{i<j}^{q-2}\sum_{j<k}^{q-1}\sum_{k}^{q}\beta_{ijjk}x_i x_j^2 x_k+\sum_{i<j}^{q-2}\sum_{j<k}^{q-1}\sum_{k}^{q}\beta_{ijkk}x_i x_j x_k^2 \quad (1)$$

The Analysis of variance (ANOVA) implies that the model is significant. However, the diagnosis of the statistical properties of the assumed model found that the distribution of residuals is not normal and that it is necessary to transform the mathematical model in order to meet the conditions of normality. The Box-Cox diagnostics (Box and Draper, 2006; Myers *et al.*, 2009) recommends a "Square Root" transformation for the variance stabilization.

The Model summary statistics for "Square Root" model transformation are suggested Special Quartic Mixture Model. Again using the Analysis of variance (ANOVA) sugested model was checked. Value such as F factor, p-value and R-squared are statistical value which are important in way of searching a best model. According to the statistic calculation the highest value of the R-squared, F factor and low value of p-value factor (p value should be lower then 0.0001) justified the model. Obtained value for F and R for the Special Quartic Mixture Model for ternary Al-Cu-Sb system are F=86.26 and R-Squared=0.931. Which are in comparison with F and R value for other models significantly higher and chosen model is justified. Same check was done for ternary Bi-Ge-Sb and obtained value for F=526.34 and R-Squared=0.9827 which also justified chosen Special Quartic Mixture Model.

For both ternary systems Al-Cu-Sb and Bi-Ge-Sb same mathematichal model were used and same procedure was applied.

The final equation of the predictive model for Bi-Ge-Sb system is given as Eq. (2):

$$\sigma(MS/m)=0.10379\cdot x(Ge)+2.42157\cdot x(Sb)+0.79146\cdot x(Bi)-3.62962\cdot x(Ge)\cdot x(Sb)-0.67350\cdot x(Ge)\cdot x(Bi)-1.73372\cdot x(Sb)\cdot x(Bi)+19.86619\cdot x(Ge)^2\cdot x(Sb)\cdot x(Bi)-18.00847\cdot x(Ge)\cdot x(Sb)^2\cdot x(Bi)\ 12.56262\cdot x(Ge)\cdot x(Sb)\cdot x(Bi)^2 \quad (2)$$

The final equation of the predictive model for Al-Cu-Sb system is given as Eq. (3):

$$\sigma(MS/m)=6.16441\cdot x(Al)+1.75798\cdot x(Sb)+7.20364\cdot x(Cu)-4.36419\cdot x(Al)\cdot x(Sb)-6.04817\cdot x(Al)\cdot x(Cu)-24.18610\cdot x(Sb)\cdot x(Cu)-58.87562\cdot x(Al)^2\cdot x(Sb)\cdot x(Cu)+86.92209\cdot x(Al)\cdot x(Sb)^2\cdot x(Cu) \quad (3)$$

TABLE 2. Electrical conductivity of the alloy from ternary Bi-Ge-Sb and Al-Cu-Sb systems

Number	Composition of sample (at.%)	Electrical conductivity (MS/m) Values for different measurement 1	2	3	4	5	Mean value
1	$Bi_{50}Sb_{50}$	1.1865	1.1744	1.1754	1.1706	1.1736	1.1761
2	$Bi_{40}Ge_{20}Sb_{40}$	0.3782	0.3767	0.3089	0.3154	0.379	0.35164
3	$Bi_{30}Ge_{40}Sb_{30}$	0.3334	0.3437	0.3118	0.2739	0.316	0.31576
4	$Bi_{20}Ge_{60}Sb_{20}$	0.266	0.2396	0.2492	0.2479	0.2656	0.25366
5	$Bi_{10}Ge_{80}Sb_{10}$	0.1879	0.1987	0.2019	0.1829	0.1889	0.19206
	Ge_{100}						0.002
6	$Bi_{50}Ge_{50}$	0.3005	0.2495	0.2598	0.2698	0.2987	0.27566
7	$Bi_{40}Ge_{40}Sb_{20}$	0.1987	0.1903	0.2013	0.189	0.2056	0.19698
8	$Bi_{30}Ge_{30}Sb_{40}$	0.3077	0.2376	0.2532	0.3085	0.3226	0.28592
9	$Bi_{22.5}Ge_{22.5}Sb_{55}$	0.6067	0.6103	0.6146	0.5752	0.6257	0.6065
10	$Bi_{20}Ge_{20}Sb_{60}$	0.8105	0.821	0.8065	0.8113	0.7889	0.80764
11	$Bi_{10}Ge_{10}Sb_{80}$	1.444	1.433	1.427	1.44	1.439	1.4366
	Sb_{100}						2.5000
12	$Ge_{50}Sb_{50}$	0.3487	0.3398	0.3402	0.3494	0.3509	0.3458
13	$Bi_{20}Ge_{40}Sb_{40}$	0.3576	0.2743	0.3465	0.3833	0.3527	0.34288
14	$Bi_{40}Ge_{30}Sb_{30}$	0.3897	0.3879	0.4298	0.3786	0.399	0.397
15	$Bi_{60}Ge_{20}Sb_{20}$	0.4319	0.4222	0.4231	0.4207	0.4021	0.42
16	$Bi_{80}Ge_{10}Sb_{10}$	0.5698	0.5598	0.5823	0.5598	0.5987	0.57408
	Bi_{100}						0.77
17	$Al_{50}Sb_{50}$	7.9833	7.8874	7.9884	7.8474	7.4354	7.8283
18	$Al_{40}Sb_{40}Cu_{20}$	5.9883	5.0999	5.8453	5.8343	5.9182	5.7372
19	$Al_{30}Sb_{30}Cu_{40}$	4.3758	4.3763	4.3792	4.3801	4.3778	4.3778
20	$Al_{20}Sb_{20}Cu_{60}$	7.9883	6.9002	7.5455	7.8876	5.0877	7.0818
21	$Al_{10}Sb_{10}Cu_{80}$	14.9875	13.9804	12.9887	14.0232	15.0011	14.1961
	Cu_{100}						59
22	$Al_{50}Cu_{50}$	28.8723	26.9893	27.7759	23.9874	29.8750	27.4999
23	$Al_{40}Sb_{20}Cu_{40}$	2.9872	2.9310	2.9857	3.0974	3.1121	3.0226
24	$Al_{30}Sb_{40}Cu_{30}$	0.4621	0.4617	0.4504	0.4593	0.4583	0.4583
25	$Al_{20}Sb_{60}Cu_{20}$	0.7613	0.7493	0.7016	0.7291	0.7353	0.7353
26	$Al_{10}Sb_{80}Cu_{10}$	1.1270	1.1080	1.1070	1.1270	1.1172	1.1172

Based on defined models electrical conductivity were predicted for all other alloys in the ternary systems and iso-lines for electrical conductivity of alloys defined by Eq. (2) and Eq. (3) are shown in Fig. 1 (a and b) respectively.

Some of the obtained light optical micrographs are presented in Fig. 2. All alloy samples from ternary Bi-Ge-Sb system have same three (Bi)+(Sb)+(Ge) phases in structure.

From micrographs presented on Fig. 2, is clearly visible that all samples are from three phase region. For better insight into microstructure two additionally samples per ternary system are investigated with SEM-EDS and XRD techniques. Obtained results are presented in Table 3. Microstructure of other samples which are not presented on Fig. 2, are presented in Table 4. All microstructures of samples from ternary Al-Cu-Sb are given in Fig. 2.

Experimentally results of XRD are compared with literature data. Literature value for lattice parameters of solid solution (Bi) are a=b=4.546 Å and c=11.862 Å defined by Cucka and Barrett (1962). Lattice parameter for solid solution (Sb) are compared with data given by Barrett *et al.* (1963), a=b=3.301 Å and c=11.232 Å. Obtained result for (Bi) and (Sb) solid solution are in reasonable agreement with literature, small deviation is visible because of solubility Sb in Bi and conversely. Data for (Ge) are used from Swanson and Tatge (1953) were determined lattice parameter are a=b=c=5.658 Å.

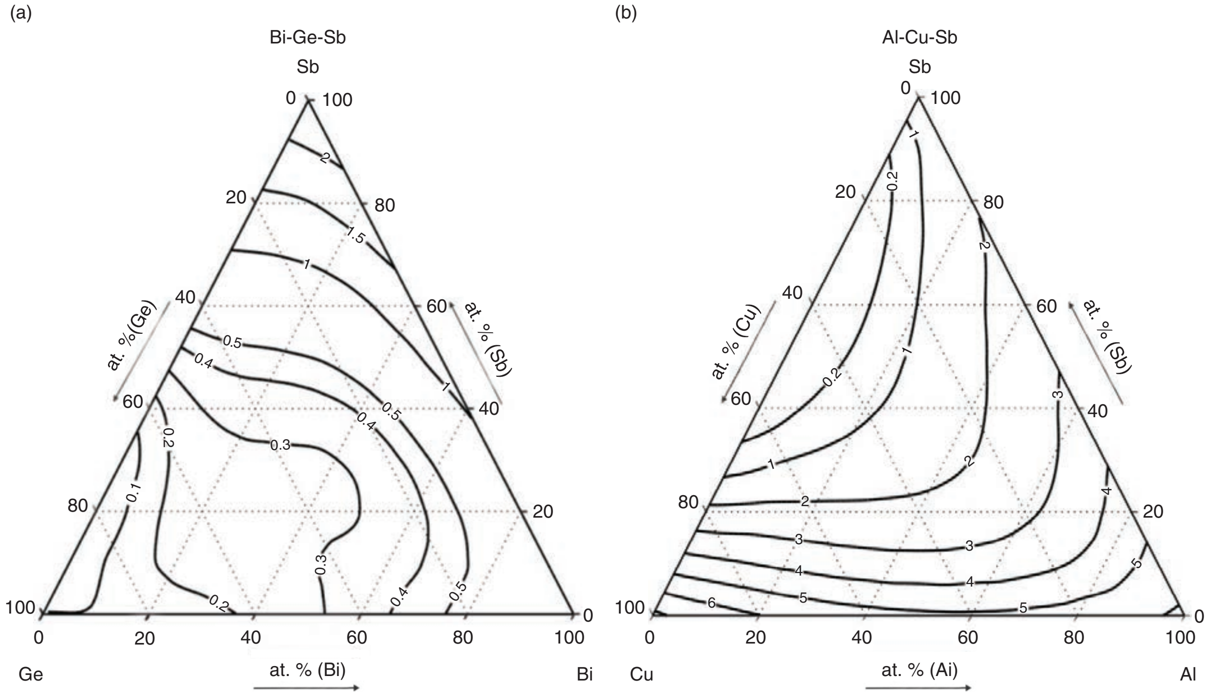

FIGURE 1. Iso-lines of electrical conductivity for the ternary: a) Bi-Ge-Sb (left), and b) Al-Cu-Sb (right) systems.

Three detected intermetallic phases AlSb, Al_4Cu_9 and Cu_2Sb from Al-Cu-Sb system are in good agreement with data given by Woolley and Smith (1958), Westman (1965), and Pearson (1985) respectively. In Fig. 3 are presented two SEM microstructure for samples A and B (see Table 3). On both micrographs are visible three phases region. Sample A rich with (Ge) formed structure with three solid solution (Bi) light phases, (Sb) grey and (Ge) darkest phase. On micrographs from LOM (see Fig. 2) is hard to notice difference between (Sb) and (Bi) phases and on SEM micrographs phases are clearly visible. Sample B belongs to three phases region (Sb)+AlSb+Cu_2Sb.

Alloy samples from ternary Bi-Ge-Sb are further investigated with micro-Vickers hardness test and results of test are shown in Table 4. Each phase was tested several times (from ten up to twenty) at different position and mean value of hardness are given in Table 4 with micrographs after testing.

Experimentally obtained hardness for solid solution (Ge) is in the range of values from 844.78 $MN.m^{-2}$ to 860.22 $MN.m^{-2}$. In microstructures is very difficult to distinguish solid solution (Bi) from solid solution (Sb) and hardness of this two phases is determined as a harness of (Bi)+(Sb) solid solution with value in the range from 64.992 $MN.m^{-2}$ to 110.244 $MN.m^{-2}$. This big difference in hardness is possible to justify by quantity of Bi and Sb in alloy. Alloys rich with Sb have a higher value of hardness than alloys rich with Bi.

4. CONCLUSIONS

- This paper presents experimental results of microstructure, electrical properties and mechanical properties of alloy from two ternary systems.
- Ternary Bi-Ge-Sb system has been investigated with a large number of sample using different experimental techniques. In microstructure of all samples were detect three solid solution (Bi), (Ge) and (Sb). All samples from three different vertical section belong to three phases region (Bi)+(Ge)+(Sb). Using SEM-EDS technic has been determined composition of the samples and phases presented in microstructure. Using XRD techniques lattice parameters were determined and confirmed phases detect with SEM-EDS. Micro-Vickers hardness test used for determination of the phase hardness detected in microstructure in the ternary Bi-Ge-Sb alloy samples. Each detected phase were tested several times at different position and determined mean value from all measurement for solid solution (Ge) is 852.8267 $MN.m^{-2}$ and for solid solution (Bi)+(Sb) is 85.06631 $MN.m^{-2}$.
- Ternary Al-Cu-Sb system was investigated with same experimental techniques as a ternary Bi-Ge-Sb system except determination of phase hardness. Using SEM-EDS and XRD techniques two alloy samples were investigated and in their structure were determined three

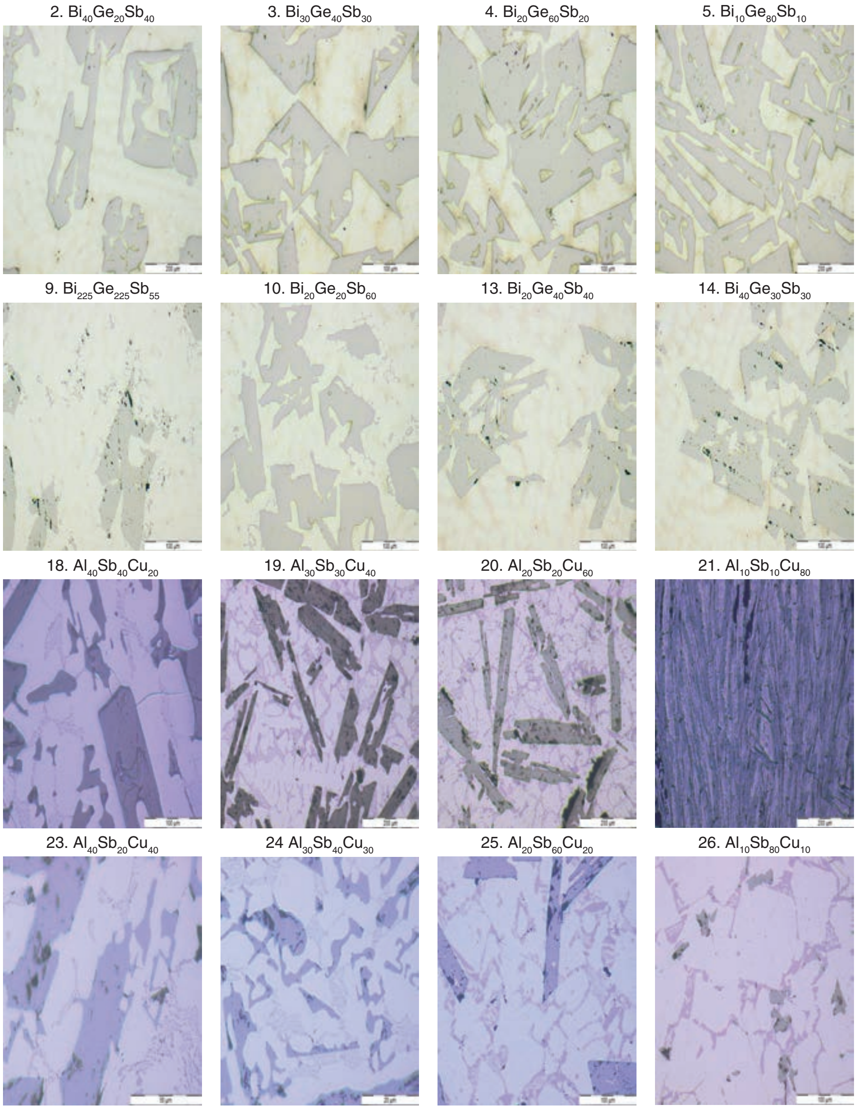

FIGURE 2. Microstructures for the selected alloys samples.

TABLE 3. Experimentally determined phase compositions and lattice parameters of the ternary Bi-Ge-Sb and Al-Cu-Sb systems

S	Overall composition (at.%)	Experiment. determined phases	Compositions of phases (at.%)					Lattice parameters (Å)	
			Bi	Ge	Al	Cu	Sb	*a=b*	*c*
A	12.03 Bi	(Bi)	86.2±.1	0.7±.2			13.1±.2	4.5285(1)	11.8576(2)
	74.58 Ge	(Ge)	0.3±.3	99.1±.3			0.6±.7	5.6503(3)	-
	13.39 Sb	(Sb)	8.8±.4	0.7±.2			90.5±.3	3.9287(2)	11.2455(2)
B	9.21 Al	AlSb			49.3±.3	0.5±.1	50.2±.1	6.1393(5)	-
	11.03 Cu	Sb			0.7±.5	0.6±.8	98.7±.8	3.3548(1)	11.2315(8)
	79.76 Sb	Cu_2Sb			0.6±.2	66.8±.6	32.6±.5	4.0324(7)	6.1159(6)
C	27.15 Bi	(Bi)	85.0±.5	0.9±.3			14.1±.4	4.5334(2)	11.8543(3)
	45.01 Ge	(Ge)	1.1±.1	98.3±.1			0.6±.3	5.6499(1)	-
	27.84 Sb	(Sb)	7.9±.2	0.5±.6			91.6±.4	3.9898(5)	11.2403(1)
D	23.73 Al	AlSb			50.6±.7	0.6±.5	48.8±.2	6.1345(4)	-
	55.52 Cu	Cu_2Sb			0.9±.1	65.3±.3	33.8±.5	4.0087(9)	6.1059(9)
	20.75 Sb	Al_4Cu_9			28.7±.4	70.5±.1	0.8±.1	8.7098(1)	-

TABLE 4. Measured Vickers microhardness of the phases in the ternary Bi-Ge-Sb system

micrographs	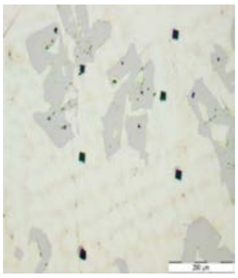		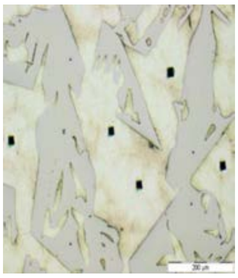		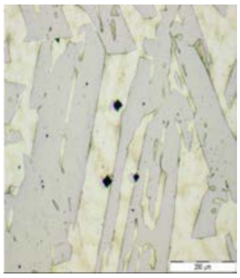		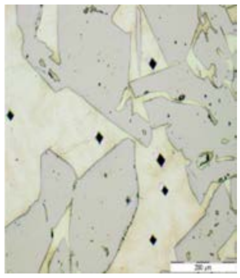	
sample	2. $Bi_{40}Ge_{20}Sb_{40}$		3. $Bi_{30}Ge_{40}Sb_{30}$		4. $Bi_{20}Ge_{60}Sb_{20}$		5. $Bi_{10}Ge_{80}Sb_{10}$	
phases	(Bi)+(Sb)	(Ge)	(Bi)+(Sb)	(Ge)	(Bi)+(Sb)	(Ge)	(Bi)+(Sb)	(Ge)
hardness ($MN.m^{-2}$)	94.17	844.78	85.56	858.98	81.854	849.64	68.738	856.8
micrographs	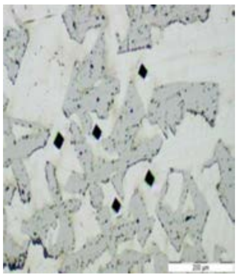		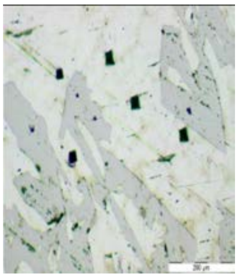		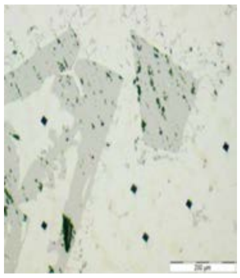		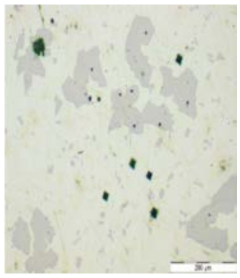	
sample	7. $Bi_{40}Ge_{40}Sb_{20}$		8. $Bi_{30}Ge_{30}Sb_{40}$		9. $Bi_{22.5}Ge_{22.5}Sb_{55}$		10. $Bi_{20}Ge_{20}Sb_{60}$	
phases	(Bi)+(Sb)	(Ge)	(Bi)+(Sb)	(Ge)	(Bi)+(Sb)	(Ge)	(Bi)+(Sb)	(Ge)
hardness ($MN.m^{-2}$)	68.738	845.46	80.366	849.64	83.912	853.44	89.07	852.18
micrographs	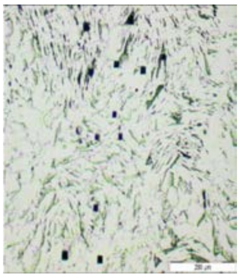		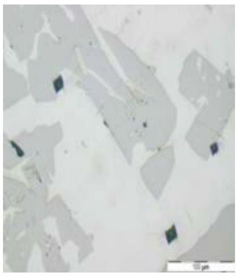		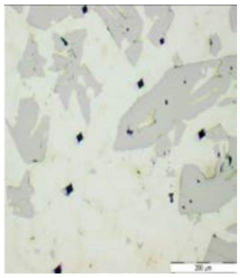		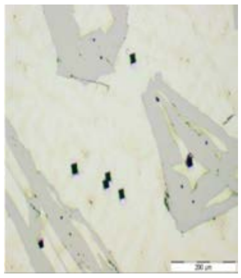	
sample	11. $Bi_{10}Ge_{10}Sb_{80}$		13. $Bi_{20}Ge_{40}Sb_{40}$		14. $Bi_{40}Ge_{30}Sb_{30}$		15. $Bi_{60}Ge_{20}Sb_{20}$	
phases	(Bi)+(Sb)	(Ge)+(Bi)+(Sb)	(Bi)+(Sb)	(Ge)	(Bi)+(Sb)	(Ge)	(Bi)+(Sb)	(Ge)
hardness ($MN.m^{-2}$)	110.244	166.92	94.17	860.22	96.292	855.48	87.756	851.58
micrographs	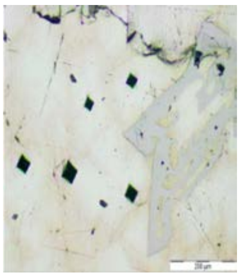							
sample	16. $Bi_{80}Ge_{10}Sb_{10}$							
phases	(Bi)+(Sb)	(Ge)						
hardness ($MN.m^{-2}$)	64.992	855.72						

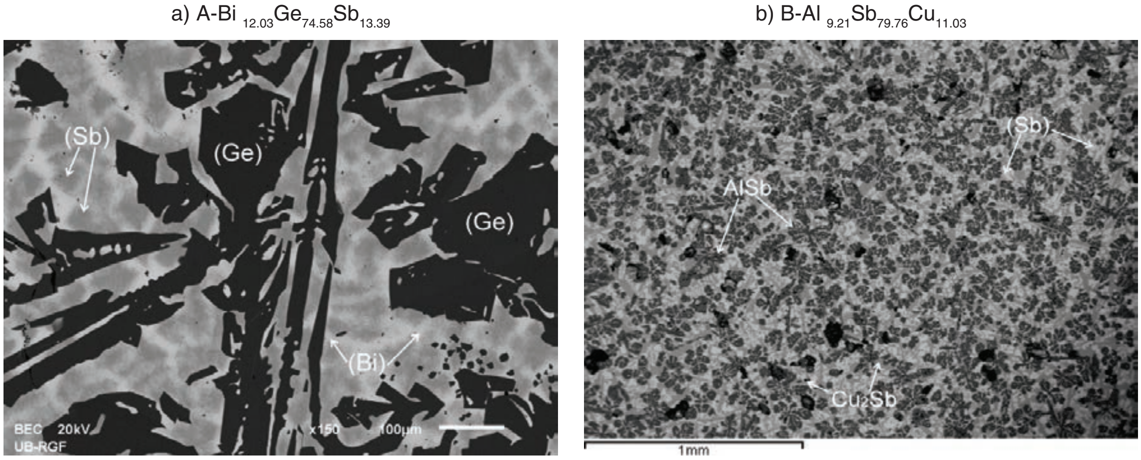

FIGURE 3. SEM micrographs for samples: a) A-$Bi_{12.03}Ge_{74.58}Sb_{13.39}$ (left), and b) B-$Al_{9.21}Sb_{79.76}Cu_{11.03}$ (right).

phases region in sample B, AlSb+Sb+Cu_2Sb and AlSb+Cu_2Sb+Al_4Cu_9 in sample D. Other prepared samples from two vertical sections are observed with light optical microscopy. In obtained micrographs are clearly visible that all samples belong to the three phase region.

– Electrical conductivity for alloys from both ternary systems and electrical conductivity for binary alloy (BiGe, GeSb, BiSb, AlSb and AlCu) have been measured. Obtained results show that ternary alloy $Bi_{10}Ge_{10}Sb_{80}$ have highest value for electrical conductivity from other ternary alloy in ternary Bi-Ge-Sb system. On the other hand results of the conductivity for alloy samples from ternary Al-Cu-Sb system were in a wide range of value from 0.4583 MS/m up to 14.1961 MS/m. The highest value of the electrical conductivity was obtained for ternary alloy $Al_{10}Sb_{10}Cu_{80}$. Besides experimental work using appropriated mathematical model has been calculated electrical conductivity for all other possible ternary alloy and results are presented as a iso-lines of electrical conductivity.

ACKNOWLEDGMENTS

This work was supported by the Ministry of Education, Science and Technological Development of the Republic of Serbia, under Project No. ON172037 and TR37020.

REFERENCES

Barrett, C.S., Cucka, P., Haefner, K. (1963). The crystal structure of antimony at 4.2, 78 and 298° K. *Acta Crystallogr.* 16, 451-453. http://dx.doi.org/10.1107/S0365110X63001262.

Bech, J., Corrales, I., Tume, P., Barceló, J., Duran, P., Roca, N., Poschenrieder, C. (2012). Accumulation of antimony and other potentially toxic elements in plants around a former antimony mine located in the Ribes Valley (Eastern Pyrenees). *J. Geochem. Explor.* 113, 100-105. http://dx.doi.org/10.1016/j.gexplo.2011.06.006.

Box, G., Draper, N. (2006). *Response Surfaces, Mixtures, and Ridge Analyses*. 2nd Ed., John Wiley and Sons, Inc., New Jersey.

Cornell, J.A. (1990). *Experiments with Mixtures. Designs, Models, and the Analysis of Mixtures Data.* 2nd Ed., John Wiley and Sons, Inc., New York.

Cucka, P., Barrett, C.S. (1962). The crystal structure of Bi and of solid solutions of Pb, Sn, Sb and Te in Bi. *Acta Crystallogr.* 15, 865-872. http://dx.doi.org/10.1107/S0365110X62002297.

Cui, X.D., Wang, Y.J., Hockmann, K., Zhou, D.M. (2015). Effect of iron plaque on antimony uptake by rice (Oryza sativa L.). *Environ. Pollut.* 204, 133-140. http://dx.doi.org/10.1016/j.envpol.2015.04.019.

Gierlotka, W. (2014). A new thermodynamic description of the binary Sb-Zn system. *J. Min. Metall. Sect. B-Metall. B* 50 (2), 149-155. http://dx.doi.org/10.2298/JMMB131103020G.

Guo, C., Li, C., Du, Z. (2016). Thermodynamic modeling of the Ga–Pt–Sb system. *Calphad* 52, 169-179. http://dx.doi.org/10.1016/j.calphad.2016.01.001.

Gray, T., Mann, N., Whitby, M. (2013). *Electrical Conductivity of the elements*. Available at http://periodictable.com/Properties/A/ElectricalConductivity.an.html (accesses 24.01.2016).

He, M., Wang, X., Wu, F., Fu, Z. (2012). Antimony pollution in China. *Sci. Total Environ.* 421-422, 41-50. http://dx.doi.org/10.1016/j.scitotenv.2011.06.009.

Illescas, S., Fernández, J., Asensio, J., Sánchez-Soto, M., Guilemany, J.M. (2009). Study of the mechanical properties of low carbon content HSLA steels. *Rev. Metal.* 45 (6), 424-431. http://dx.doi.org/10.3989/revmetalm.0902.

Johnson, C.A., Moench, H., Wersin, P., Kugler, P., Wenger, C. (2005). Solubility of antimony and other elements in samples taken from shooting ranges. *J. Environ. Qual.* 34 (1), 248-254.

Kolarević, M. (2004). *Rapid product development.* Ed. Foundation Andrejevic, Belgrad.

Lazić, Ž. (2004). *Design of Experiments in Chemical Engineering: Practical Guide*. Ed. Wiley-VCH Verlag GmbH & Co.KGaA, Weiheim, Alemania. http://dx.doi.org/10.1002/3527604162.

Liu, Y., Xu, J., Kang, Z., Wang, J. (2013). Thermodynamic descriptions and phase diagrams for Sb–Na and Sb–K binary systems. *Thermochim. Acta* 569, 119-126. http://dx.doi.org/10.1016/j.tca.2013.07.009.

Macgregor, K., MacKinnon, G., Farmer, J., Graham, M. (2015). Mobility of antimony, arsenic and lead at a former antimony mine, Glendinning, Scotland. *Sci. Total Environ.* 529, 213-222. http://dx.doi.org/10.1016/j.scitotenv.2015.04.039.

Minić, D., Premović, M., Cosović, V., Manasijević, D., Živković, D., Kostov, A., Talijan, N., (2013). Experimental investigation and thermodynamic calculations of the Al–Cu–Sb phase diagram. *J. Alloy Compd.* 555, 347-356. http://dx.doi.org/10.1016/j.jallcom.2012.12.059.

Myers, R.H., Montgomery, D.C., Anderson-Cook, C.M. (2009). *Response Surface Methodology: Process and Product Optimization Using Designed Experiments.* 3rd Ed., John Wiley and Sons, New Jersey, p. 704.

Pearson, W.B. (1985). The Cu_2Sb and related structures. *Z. Kristallogr.* 171, 23-39. https://doi.org/10.1524/zkri.1985.171.14.23.

Pierart, A., Shahid, M., Séjalon-Delmas, N., Dumat, C. (2015). Antimony bioavailability: Knowledge and research perspectives for sustainable agricultures. *J. Hazard. Mater.* 289, 219-234. https://doi.org/10.1016/j.jhazmat.2015.02.011.

Premović, M., Minić, D., Cosović, V., Manasijević, D., Živković, D. (2014). Experimental investigation and thermodynamic calculations of the Bi-Ge-Sb phase diagram. *Metall. Mater. Trans. A* 45(11), 4829-4841. http://dx.doi.org/10.1007/s11661-014-2445-4.

Serrano, N., Díaz-Cruz, J.M., Ariño, C., Esteban, M. (2016). Antimony- based electrodes for analytical determinations. *Trends Analyt. Chem.* 77, 203-213. http://dx.doi.org/10.1016/j.trac.2016.01.011.

Sun, W., Xiao, E., Dong, Y., Tang, S., Krumins, V., Ning, Z., Sun, M., Zhao, Y., Wu, S., Xiao, T., (2016). Profiling microbial community in a watershed heavily contaminated by an active antimony (Sb) mine in Southwest China. *Sci. Total Environ.* 550, 297-308. http://dx.doi.org/10.1016/j.scitotenv.2016.01.090.

Swanson, H.E., Tatge, E. (1953). *Standard X-ray diffraction powder patterns*. Vol. 1, National Bureau of Standards, USA, pp. 1-95.

Verbeken, K., Infante-Danzo, I., Barros-Lorenzo, J., Schneider, J., Houbaert, Y. (2010). Innovative processing for improved electrical steel properties. *Rev. Metal.* 46(5), 458-468. http://dx.doi.org/10.3989/revmetalm.1010.

Vinhal, J., Gonçalves, A., Cruz, G., Cassella, R. (2016). Speciation of inorganic antimony (III & V) employing polyurethane foam loaded with bromopyrogallol red. *Talanta* 150, 539-545. https://doi.org/10.1016/j.talanta.2015.12.080.

Westman, S. (1965). Refinement of the gamma - Cu_9Al_4 structure. *Acta Chem. Scand.* 19, 1411-1419. http://dx.doi.org/10.3891/acta.chem.scand.19-1411.

Woolley, J.C., Smith, B.A. (1958). Solid solution in A(III) B(V) compounds. *Proc. Phys. Soc.* 72(2), 214-223. http://dx.doi.org/10.1088/0370-1328/72/2/306.

Zobač, O., Sopoušek, J., Kroupa, A. (2015). Calphad-type assessment of the Sb–Sn–Zn ternary system. *Calphad* 51, 51-56. http://dx.doi.org/10.1016/j.calphad.2015.08.002.